

# DRAFT PAPER

7th Middle East NDT Conference & Exhibition  
Gulf International Convention Center, Gulf Hotel  
Manama, Kingdom of Bahrain  
September 13 - 16, 2015

## IMAGING CORROSION UNDER INSULATION AND UNDER FIREPROOFING, USING MR-MWM<sup>®</sup>-ARRAY SENSORS

Neil Goldfine<sup>1</sup>, Brian Manning<sup>1</sup>, Zachary Thomas<sup>1</sup>, Yanko Sheiretov<sup>1</sup>, Scott Denenberg<sup>1</sup>, Todd Dunford<sup>1</sup>,  
Shayan Haque<sup>1</sup>, Rasheed Al Rushaid<sup>2</sup>, Frederick Haught<sup>2</sup>

<sup>1</sup>JENTEK Sensors, Inc., 110-1 Clematis Avenue, Waltham, MA 02453-7013

<sup>2</sup>Al Rushaid Technologies Co., Al Turki Business Park, Office Villa #4; 7244 King Saud Road, Ad Doha Al  
Janubiyah, Dhahran 34455, Kingdom of Saudi Arabia

**ABSTRACT.** There is a need to image internal and external corrosion for piping and vessels through insulation with metallic weather jacket and through concrete fireproofing with or without wire mesh (e.g., for refinery vessels skirts and liquid petroleum gas sphere legs). There is a similar need in shallow and deep water for inspection through concrete weight coat, wet insulation, epoxy coatings, or polymer coatings. This paper describes the MR-MWM<sup>®</sup>-Array sensor technology and recent advances in this technology for corrosion under insulation/corrosion under fireproofing (CUI/CUF). This presentation includes a summary of performance trial results for CUI and field test efforts for CUF.

### INTRODUCTION

Magnetic field based sensing methods (such as eddy current sensors) have many characteristics that make them ideal for inspecting through coatings and insulation such as non-contact operation, insensitivity to the properties of non-conductive materials (such as insulation and coatings), and the ability to measure multiple material properties simultaneously. Yet, traditional eddy current testing (ET) is limited when inspecting through thick materials or layers of different materials. As described in this paper, these limitations can be overcome by changing the design and construction of ET sensors and expanding the operating frequency range to lower frequencies. Others have implemented pulsed ET methods and saturated low frequency ET methods that overcome some of these limitations. However, existing pulsed ET methods must be operated in a stationary mode and saturated low frequency ET methods are generally very cumbersome (needing large magnets or coils to provide the saturating field). These existing methods are not robust to variations in piping conditions (e.g., available pulsed ET solutions have not successfully employed a model based methodology to correct for varying insulation thickness, weather jacket thickness, or pipe material properties). This is critical since, for example, insulation that has had moisture ingress (the cause of external corrosion) often has varying insulation

# DRAFT PAPER

thickness around the circumference, due to sagging. The impact of such insulation thickness variation on pipe wall thickness measurements can introduce large errors, without a robust model derived correction. This paper describes the MR-MWM-Array method and the associated multivariate inverse methods (MIMs) that overcome all the above limitations. To be practical this is also accomplished in a cost effective, light weight, and compact solution.

## TECHNICAL APPROACH

### MWM-Array Sensor Technology

MWM-Array sensors operate in the magnetoquasistatic regime. In this regime, which typically involves operation at frequencies under 10 MHz, the dominant behaviors are the same as eddy current sensors for the higher operating frequencies and transition to a combination of ET and magnetic circuit theory behaviors at lower frequencies. A typical schematic of a dual rectangle MWM-Array design is shown in FIGURE 1 (a). A typical depth of penetration (DOP) chart is shown in FIGURE 1 (b). For this sensor design, inductive sensing element loops (as illustrated in the left drive rectangle) can be used to measure the time rate of change of the magnetic field at multiple locations along the drive winding. These inductive sense elements are typically used at relatively high frequencies to image surface corrosion through coatings/insulation or to measure the depth of and map out stress corrosion cracks (SCC) in SCC colonies.

Inductive sensing elements can provide high resolution images when operating at relatively high frequencies. For inductive sensors, the response is proportional to the rate of change of the magnetic fields (which goes down as the frequency is lowered). As shown in Figure 1(b), to achieve deeper penetration and detect internal corrosion, the MWM-Array must operate at lower frequencies. At these lower frequencies, the inductive sensing elements lose sensitivity. Note that at lower frequencies, the MWM-Array, as with other magnetic field ET based methods, will lose substantial resolution compared to the higher frequency response. Thus, it is generally possible to provide very high resolution corrosion imaging only for external corrosion, at high frequencies, when the depth of penetration is shallow. Furthermore, when there is no weather jacketing, it is possible to work at even higher frequencies, providing even higher external corrosion imaging resolution.

Magnetoresistive solid state sensing elements (as illustrated within the right drive rectangle in Figure 1(a)) provide much better performance at low frequencies and enable imaging of internal corrosion through the weather jacket, through the insulation, and finally through the pipe wall. These sensors measure the magnetic field itself and provide dramatically improved signal-to-noise for the response to damage at low frequencies. [1, 2]. The DOP chart illustrates the underlying behavior difference between skin effects that limit the depth of penetration at higher frequencies (as for conventional ET sensors) and the magnetic circuit and Laplacian decay behavior that dominates the lower frequency responses. At lower frequencies, the drive winding geometry (characterized by the spatial wavelength,  $\lambda$ ) and the drive-to-sense element gap limit the depth of penetration. The low frequency limit

# DRAFT PAPER

is  $\lambda/2\pi$ ; thus, to inspect through thick insulation and pipe walls a large drive winding is needed.

MWM sensor design, fabrication, and data processing is based on understanding gained from physics-based modelling. By producing sensors that match responses predicted by the models, advanced calibration and data processing techniques can be used to convert the sensor response into relevant pipe wall properties of interest (such as pipe wall thickness) independent of other factors that would confuse other methods (such as changes in sensor lift-off or insulation thickness).

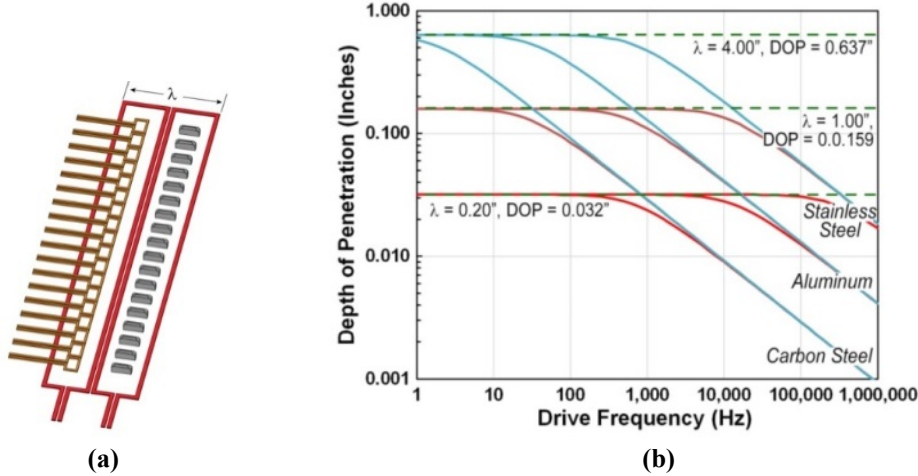


FIGURE 1. (a) Schematic of an MWM-Array with a single linear drive winding (red) and multiple sense elements. This type of sensor can use inductive sense elements (brown, MWM-Array) or magneto-resistive sense elements (grey, MR-MWM-Array). The spatial wavelength ( $\lambda$ ) of the sensor is defined in the schematic at left. (b) The Depth of Penetration (DOP) chart for three materials and three MWM-Array sensors.

## Measurement and Data Processing

An advantage of the MWM-Array geometry is that the sensor responses can be accurately predicted using uniform (or linearly varying) layered media models. The inputs to the model are the sensor's key dimensions (e.g., spatial wavelength, drive-sense gap), and the values of the material under test (MUT) properties (including the permeability, conductivity, and thickness of the steel, and the sensor lift-off). Given these inputs, the sensor response can be predicted accurately over the ranges of possible MUT properties and sensor lift-off that are anticipated for the inspection application. These responses are stored in precomputed databases called grids (for 2-unknowns), lattices (for 3-unknowns) and hyperlattices (for four or more unknowns).

MWM and MWM-Array responses are converted into material properties, layer thicknesses and lift-off estimates using a MIM [3, 4], implemented in software, using a very rapid multi-dimensional searching algorithm that has been developed and enhanced based on experience over nearly three decades. To estimate two properties, two equations are needed. This is a non-linear algebra problem for a complex multivariate partial differential equation. As in linear algebra at least two equations are needed to solve for

# DRAFT PAPER

2-unknowns and three equations for 3-unknowns and so on. At a single frequency, the impedance measurement provides two equations (i.e., the magnitude and phase are each a function of the MUT properties and sensor geometry). The magnitude and phase of the impedance can also be represented in terms of the real and imaginary parts of the complex impedance. It is generally preferred to do the MIM searching within a database of responses for the complex impedance terms instead of the magnitude and phase. This is simply because magnitude and phase have different units, while the real and imaginary parts have the same dimensions (or if normalized can be made dimensionless). Thus in summary, for a three unknown problem such as internal corrosion on a pipe with no coating (where the unknowns might be the magnetic permeability of the pipe, the thickness of the pipe and the lift-off), two frequencies are needed to provide four equations to solve for the three unknowns. For a more complex problem with a weather jacket and insulation, there are at least five unknowns (lift-off distance to the weather jacket, thickness of the weather jacket, insulation thickness, pipe wall thickness and pipe wall magnetic permeability). Note it is practical to assume the conductivity of the weather jacket and pipe wall are known (or are determined at a location of assumed nominal pipe wall thickness). For this five unknowns CUI application, three frequencies are needed. These frequencies must be carefully selected so that independent measurement of each unknown is possible.

FIGURE 2 and FIGURE 3 shows examples of lattices for this five unknown application, where some properties are assumed constant so that we can visualize the databases. The size of the quadrilaterals formed by four grid points within the grids represents the sensitivity to the two properties represented by each grid within the lattice. The orthogonality of the grid lines represents the ability to measure the displayed properties independently. The more orthogonal (closer to 90 degrees) the lines are, the more independent the measurements can be. However, MIMs perform well even with the grid lines are far from orthogonal. This allows the MWM-Arrays to operate over a wider frequency range, enabling solutions to many challenging problems.

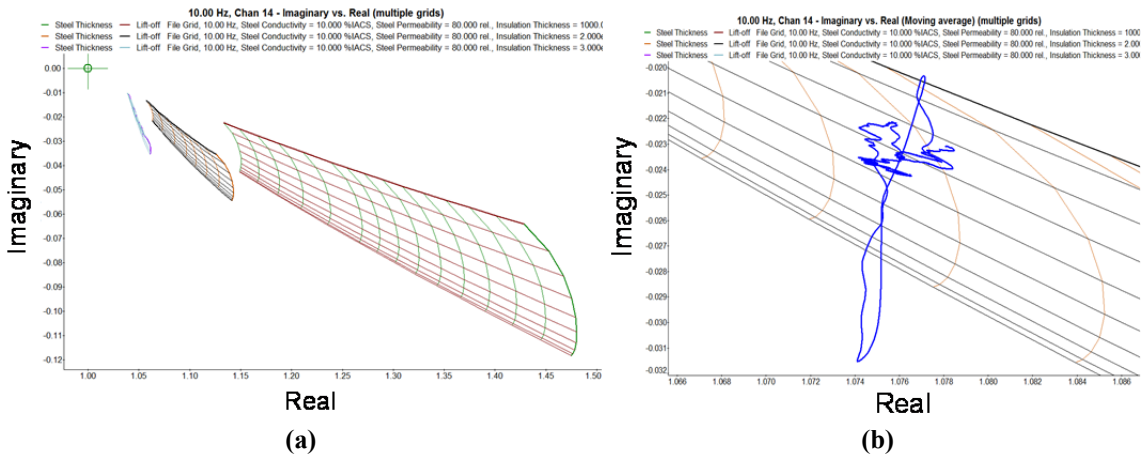
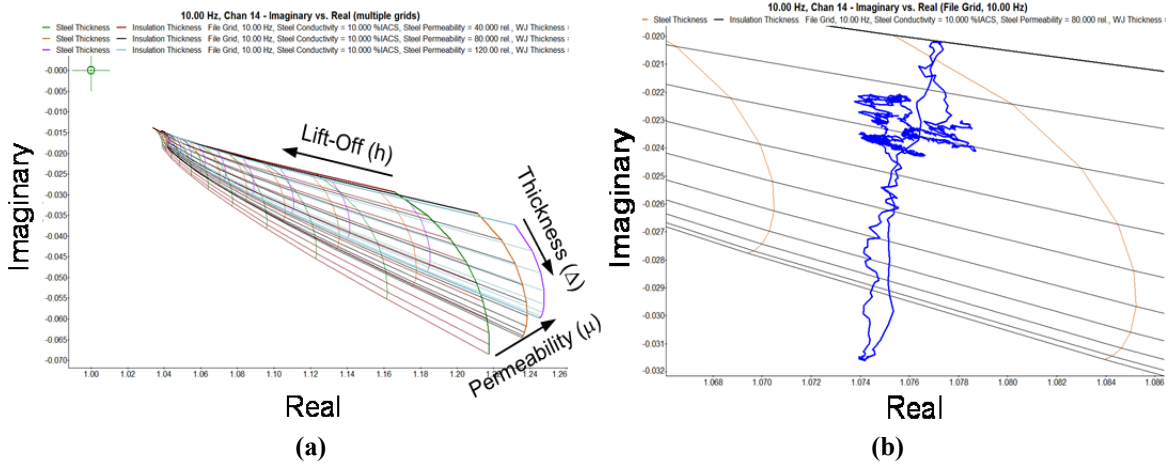


FIGURE 2. (a) Lattice visualizations for grids of pipe wall thickness and lift-off, where each grid is for a different insulation thickness. Note that for this lattice visualization, the weather jacket thickness and pipe wall permeability are assumed to be constant. (b) A single grid from the lattice with an expanded view of data taken for a single MR-MWM-Array channel shown on the grid.

# DRAFT PAPER



**FIGURE 3.** (a) Lattice visualizations for grids of pipe wall thickness and lift-off, where each grid is for a different pipe wall magnetic permeability. Note that for this lattice visualization, the weather jacket thickness and insulation thickness are assumed to be constant. (b) A single grid from the lattice with an expanded view of data taken for a single MR-MWM-Array channel shown on the grid.

Note that as shown in Figure 2 (a) the change in insulation thickness produces a very large shift in the response grids (each grid is for a different insulation thickness). While as shown in Figure 3 (a) a change in magnetic permeability of the pipe wall results in a smaller change (each grid is for a different magnetic permeability). The capability to measure these properties independently will depend on how separate or distinct the response hyperlattices are for the three measurement frequencies. Note that the hyperlattices above are only for one frequency. Three different frequencies are needed to measure the five unknown properties of lift-off, weather jacket thickness, insulation thickness, pipe wall magnetic permeability, and most importantly pipe wall thickness. The more unique (and uncorrelated) the shapes of the hyperlattices at the different frequencies, the more likely it is that the properties of interest can be estimated independently.

## Calibration – Air Calibration per ASTM E2338

For insulated piping, it is not feasible to generate reference standards that encompass the wide range of piping configurations encountered in facilities. To overcome this challenge, other electromagnetic methods typically use the pipe being inspected as a calibration point. Since JENTEK's physics-based models can accurately predict the response of the MWM sensors, the calibration for MWM sensors can be performed by making a measurement in air as described in ASTM Standard E2338 [5]. This air calibration is simple to perform, which increases repeatability and reduces variability between operators. Measurements on piping are subsequently used to verify the system performance, as described in ASTM Standard E2884 [6], by ensuring that the relevant responses (such as lift-off and pipe wall thickness) are reasonable for the inspection being performed. At times it is useful to combine a calibration in air with a partial reference calibration on a section of pipe

## DRAFT PAPER

assumed to have the nominal thickness. This partial calibration on the pipe enables the method to determine the conductivity of the pipe (a sixth unknown) without assuming that the insulation thickness is known. This is often, but not always, practical.

### MWM-Array Sensor Design for CUI

When designing sensors for a given application, the sensor drive winding “spatial wavelength” is a significant design parameter. FIGURE 1 (a) shows the definition of the spatial wavelength ( $\lambda$ ) for a dual rectangle drive, MWM-Array. The spatial wavelength is an important consideration because it affects the DOP of the magnetic field into the test material. As shown in FIGURE 1 (b), the DOP depends upon the material being inspected, the drive current frequency, and sensor geometry. At high frequencies, the DOP is limited by the drive frequency and the properties of the material being inspected. However, at low frequencies, the DOP is limited by the sensor geometry. For a CUI application, the magnetic fields from a larger spatial wavelength sensor will penetrate farther into the MUT than a shorter spatial wavelength sensor (note that the field decays within the insulation at all frequencies due to Laplacian decay associated with the winding geometry). While the drive frequency can be varied by the instrumentation, the spatial wavelength is part of the sensor design and must be determined in advance. In order to inspect through the thickness of a carbon steel pipe and through a thick layer of insulation, the sensors must have a sufficiently large spatial wavelength and be driven at sufficiently low frequencies (see FIGURE 1).

Operating the sensors at very low frequencies is challenging. Magnetoresistive (MR) sense elements have relatively high sensitivity (compared to inductive sensing elements) at these low frequencies, since their sensitivity to the magnetic flux density is independent of frequency [2, 7, 8, 9]. A new instrument and probe electronics unit was designed specifically to meet the challenges of delivering the required signal-to-noise and in a fully parallel architecture configuration that also enable rapid data acquisition [2, 10, 11, 12, 13]. This, and other enhancements, allows the MR-MWM-Array to operate in a scanning mode rather than taking stationary point measurements.

### PERFORMANCE EVALUATION

FIGURE 4 (a) shows an earlier generation MR-MWM-Array Corrosion Imaging Tool used for the initial performance evaluations. These blind tests were performed on corrosion samples made accessible by a major oil company. The testing was performed at a research and testing facility in Houston, TX. The samples were 20-in. pipes (508mm) with 0.250-in. (6.35mm) wall thickness. These pipes were insulated with 2-in. (50.8mm) insulation and 0.020-in. (0.51mm) thick aluminum weather jacket. FIGURE 4 (b) shows the 8200 $\alpha$  (Integrated) impedance instrument used during the testing. FIGURE 4 (c) shows one of the external corrosion defects that were detected and sized by the MR-MWM-Array. These were natural corrosion areas with varying sizes (length and width as well as depth).

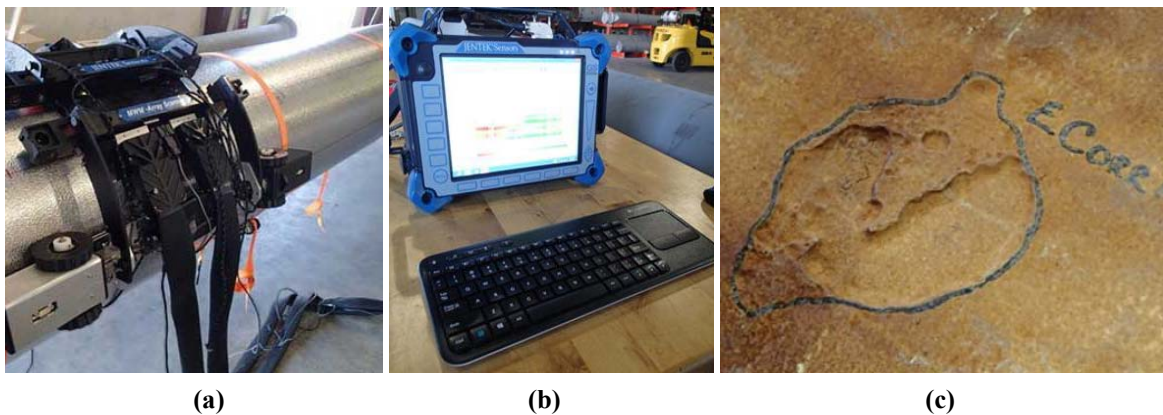
## DRAFT PAPER

TABLE 1 shows a chart of the various defects detected by the tool. Since the MR-MWM-Array technology is sensitive to the thickness of the pipe over an area that is referred to as the sensor footprint, the estimates of the pipe wall thickness as measured by the sensor are a weighted average of the actual pipe wall thickness over the footprint. As a result, defects that are narrow in either the axial or circumferential direction when compared to the sensor footprint would produce wall thickness estimates that are larger than the actual wall thickness, i.e. the flaw depths will be underestimated. Note that the footprint is larger than the actual size of the individual sense elements and defines the region that each sensing element is sensitive to on the surface of the MUT.

FIGURE 5 shows a typical C-Scan of the pipe wall thickness for one of the pipe sections. The x-axis of the C-Scan image represents the axial distance measured by the position encoder on scanner. The y-axis represents the circumferential distance of measurements performed on the pipe surface. The C-Scan represents a full circumferential map of the pipe samples with external corrosion. The “greyed out” areas represent weather jacket overlap regions where the detection performance of the MR-MWM-Array is reduced.

During the same evaluation, scans were also performed on samples with internal corrosion. The samples were 16-in. (406mm) pipes with 0.500-in. (12.7mm) pipe walls. These pipe samples were also insulated with 2-inch (50.8mm) insulation and 0.020-inch (0.51mm) thick aluminum weather jacket. A typical C-scan for an internally corroded pipe (near a weld) is shown in FIGURE 6.

Since this evaluation was performed in 2013, significant improvements have been made with regards to reducing the sensor footprint, reducing the size of the “uninspected” region due to weather jacket overlap as well as the overall detection performance of the system.



**FIGURE 4. (a) An early prototype Corrosion Imaging Tool used during one of the performance evaluations. (b) The GridStation 8200 $\alpha$  (Integrated) Impedance Instrument. (c) Close-up of an external corrosion region detected by the MR-MWM-Array.**

## DRAFT PAPER

Axial Length (inches/mm)	Circumferential Length (inches/mm)	Mean Depth (inches/mm)	Hit/Miss
1.5/38	1.50/38	0.12/3.0	Hit
9.0/228	1.50/38	0.06/1.5	Miss
2.0/50	1.50/38	0.08/2.0	Miss
4.0/101	1.25/32	0.12/3.0	Hit
4.0/101	4.00/101	0.08/2.0	Hit
4.0/101	4.50/114	0.08/2.0	Hit
1.75/44	2.75/70	0.10/2.5	Hit
2.75/69	2.50/63	0.12/3.0	Hit
1.0/25	0.75/19	0.16/4.0	Miss

**TABLE 1.** List of external corrosion areas detected by the MR-MWM-Array during a blind performance evaluation of pipe samples with natural external corrosion.

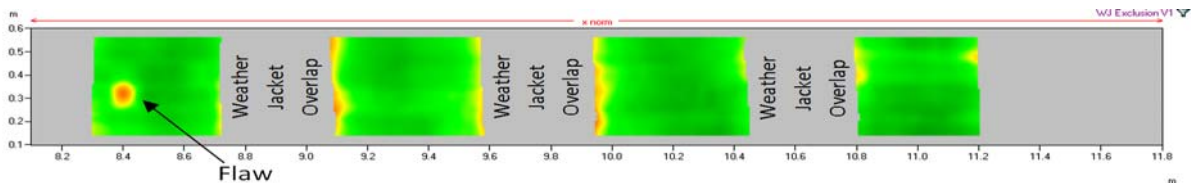


**FIGURE 5.** MR-MWM-Array C-Scan image of the wall thickness of a pipe sample with natural external corrosion. The weather jacket overlap areas have been greyed out.

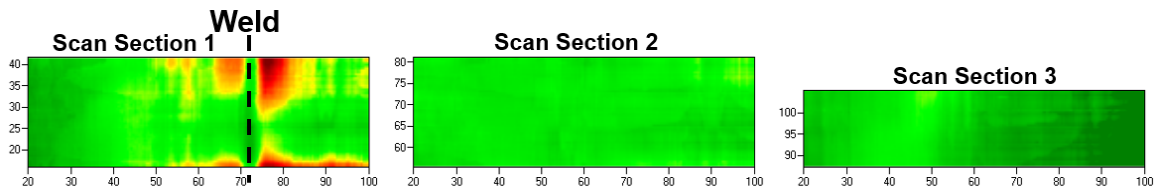


**FIGURE 6.** MR-MWM-Array C-Scan images of the wall thickness of a pipe sample with internal corrosion near a weld.

### PRELIMINARY FIELD DEMONSTRATIONS – LARGE STRUCTURES: TANKS, VESSELS, ETC.

Tanks and vessels that are insulated or have fireproofing can be inspected using the same methods as piping. The MR sensor is flexible and can be adapted for the larger diameters. However, there are several challenges that make these larger structures different in important ways. First, these structures often use thicker steel compared to piping. Second, the large diameter and large areas require different scanning strategies. Also, for fireproofing, it is necessary to model the steel mesh reinforcement.

In order to perform measurements that penetrate through the steel, the MR-MWM-Array sensor arrays must operate at low frequencies. This capability has been demonstrated in the lab for up to 0.875-in. (22.2mm) steel. The sensors can also be operated in a different mode that allows inspection for only external corrosion of thicker steels. In this case the

## DRAFT PAPER

result is a map of the shape of the external surface of the steel and corrosion would be detected using these external surface topology maps.

FIGURE 7 (a) shows a prototype MR-MWM-Array vessel scanner that was used for field demonstrations at a facility in the Middle East. The goal of these field demonstrations was to gain experience in the effectiveness of the MR-MWM-Array for the inspection of Corrosion under Fireproofing (CUF) in oil and gas facilities. Large area scans were accomplished in multiple vertical passes, with automatic scanning in the vertical direction, and then manual shifting of the scanner around the vessel. FIGURE 7 (b) shows how the scans on the vessels were performed. FIGURE 7 (c) shows the wall thickness map for the vessel.

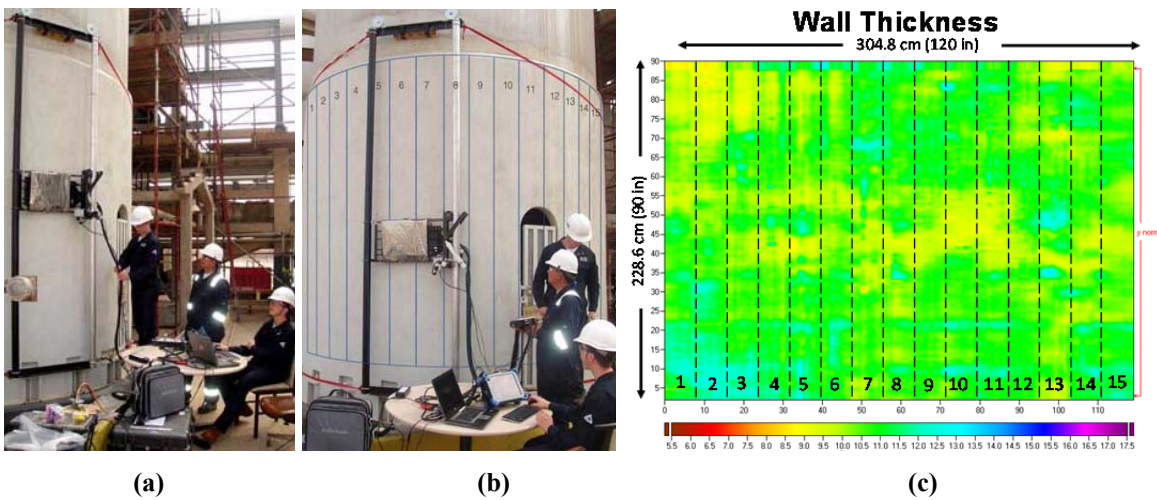


**FIGURE 7. (a) An early prototype MR-MWM-Array vessel scanner performing scans on a large vessel surface. (b) Numbered overlays illustrating how skirt wall thickness images were created from multiple vertical C-scans (c).**

## TECHNOLOGY TRANSITION

The GridStation<sup>®</sup> Corrosion Imaging Tool is currently being transitioned as a commercially-available tool for field services by non-destructive testing (NDT) service providers at two major U.S. refineries. Several field trials and demonstrations have been performed over the past two years to demonstrate capability, as well as refinements for field performance. The transition plan had three major components – (1) a thorough commercialization plan that reviews the technology status and inspection requirements, (2) development of comprehensive training information and standards to enable widespread industry adoption, and (3) maturation of manufacturing processes, including working towards ISO certification.

A comprehensive training curriculum, specifically aimed at training field technicians with limited exposure to eddy current technology, has been developed. This four-day course

## DRAFT PAPER

includes classroom instructions to students to introduce eddy current concepts, information about the scanning fixtures, selection of the sensor array configurations and operating frequencies, software configurations, measurement databases being used as well as considerations for estimating damage conditions. Additionally, the curriculum includes hands-on training on live lines and piping inside a refining or an off-plot unit. To date, more than fifteen field technicians, spread across the U.S., have been trained to perform field inspections using the Corrosion Imaging Tool. Last year coordination began with NDT service companies to provide field service support to technicians performing field inspections for corrosion under insulation at several major U.S. refineries. As shown in FIGURE 8, engineers provided initial service support to NDT field technicians using the Corrosion Imaging Tool to inspect a variety of pipes in an alkylation unit in an oil refinery. These pipes were known to operate under conditions that make CUI a likely problem. This unit was being inspected using the MR-MWM-Array sensors in advance of a shutdown so that repair work could be planned in advance without removing insulation. A large percentage of the piping in this unit was directly inspected for corrosion using the tool. This not only eliminated the need to build scaffolds or the use of man-lifts, but it also minimized the need for insulation removal and unplanned work during the next shutdown while ensuring integrity between shutdowns.



FIGURE 8. CUI pipe inspection in an alkylation unit at an oil refinery.

## CONCLUSION

The MR-MWM-Array represents the next generation of electromagnetic inspection technologies. Advancements in model-based data processing, electromagnetic simulation, and cutting-edge electronics design produce a system that can rapidly and accurately assess piping and steel structures for internal and external corrosion. The ability to provide wide-area inspections for issues such as CUI, sulfidation, naphthenic acid, erosion, and other corrosion mechanisms is essential, especially since many of these corrosion mechanisms can be driven by localized conditions that are difficult to capture using statistics-based limited inspection programs. The MR-MWM-Array ability to provide wide-area inspections for these corrosion mechanisms while the units remain in service will greatly reduce the risks to safety, equipment, and productivity.

## DRAFT PAPER

The authors and their team continue to make improvements to the MR-MWM-Array inspection system [14] and software, while expanding the applications addressed [15, 16]. New automated and manual scanners are being developed and tested for vessel inspection. Hand-held sensors are being developed that can access areas with significant interferences, such as near pipe stands, nozzles, etc. The industry need to inspect bends, T's and elbows are also being addressed. The size and weight of the system is being reduced to allow for rope access inspections. The goal is to provide a suite of inspection tools that can provide cost effective inspection of piping, vessels, and other structures throughout refineries, chemical plants, and other industrial facilities.

### ACKNOWLEDGMENTS

The technology was developed and funded by JENTEK Sensors, Inc., the U.S. Department of Transportation, and several launch customers, such as Chevron. JENTEK Sensors provided the new GridStation 8200 instruments, the MR-MWM-Arrays and the scanners to support the research and field testing described in this paper.

### REFERENCES

1. Goldfine, N.J., "Magnetometers for Improved Characterization in Aerospace Applications," *ASNT Materials Evaluation*, Vol. 51, No. 3, March 1993, pp. 396–405.
2. Goldfine, N.J., Melcher, J.R., "Magnetometer Having Periodic Winding Structure and Material Property Estimator," US Patent # 5,453,689, September 26, 1995.
3. Goldfine, N.J., Zilberstein, V.A., Schlicker, D.E., Grundy, D.C., Shay, I.C., Lyons, R.J., Washabaugh, A.P., "Hidden Feature Characterization Using a Database of Sensor Responses," US Patent # 7,161,351, January 9, 2007.
4. Sheiretov, Y.K., Goldfine, N.J., Washabaugh, A.P., Schlicker, D.E., "Material Property Estimation Using Non-Orthogonal Responsive Databases," US Patent # 7,467,057, December 16, 2008.
5. ASTM E2338, "Standard Practice for Characterization of Coatings Using Conformable Eddy-Current Sensors without Coating Reference Standards," February 2011.
6. ASTM E2884, "Standard Guide for Eddy Current Testing of Electrically Conducting Materials Using Conformable Sensor Arrays," June 2013.
7. Denenberg, S.A., "Magnetoquasistatic Sensors for Rapid Imaging of Steel Pipeline Properties," Ph.D. thesis, University of Illinois at Urbana-Champaign, 2014.
8. Sheiretov, Y., "Deep Penetration Magnetoquasistatic Sensors," Ph.D. thesis, Department of Electrical Engineering and Computer Science, Massachusetts Institute of Technology, June 2001.
9. Goldfine, N. J. and Melcher, J. R., "Apparatus and Methods for Obtaining Increased Sensitivity, Selectivity, and Dynamic Range in Property Measurements Using Magnetometers," US patent # 5,629,621, May 13, 1997.

## DRAFT PAPER

10. Shay, I.C., Goldfine, N.J.; Washabaugh, A.P., Schlicker, D.E., “Magnetic Field Sensor Having a Switchable Drive Current Spatial Distribution,” US Patent # 6,992,482, January 31, 2006.
11. Schlicker, D.E., Goldfine, N.J., Washabaugh, A.P., Walrath, K.E., Shay, I.C., Grundy, D.C., Windoloski, M., “Eddy Current Sensor Arrays Having Drive Windings with Extended Portions,” US Patent # 6,784,662, August 31, 2004.
12. Denenberg, S.A., Dunford, T.M., Goldfine, N.J., Sheiretov, Y.K., “Method and Apparatus for Inspection of Corrosion and Other Defects Through Insulation,” US Patent # 20130124109 A1, 16 May 2013.
13. Sheiretov, Y.K., Goldfine, N.J., Washabaugh, A.P., Schlicker, D.E., “Material Property Estimation Using Inverse Interpolation,” US Patent # 8,050,883, 1 November, 2011.
14. Denenberg, S., T. Dunford, Y. Sheiretov, S. Haque, B. Manning, A. Washabaugh, Neil Goldfine, “Advancements in Imaging Corrosion Under Insulation for Piping and Vessels,” *Materials Evaluation*, Vol. 73, No. 7, 2015, pp. 987–995.
15. Goldfine, N., Denenberg, S., Manning, B., Thomas, Z., Al-Rushaid, R., Haught, F., “Modeling and Visualization for Imaging of Subsurface Damage,” 7th Middle East NDT Conference & Exhibition, Manama, Kingdom of Bahrain, September 13–16, 2015.
16. Goldfine, N., Sheiretov, Y., Manning, B., Thomas, Z., Dunford, T., Denenberg, S., Al Rushaid, R., Haught, F., Bayangos, J., Minachi, A., “Inspection of Steel Vessels with Cladding Overlay, using MWM-Array Technology” 7th Middle East NDT Conference & Exhibition, Manama, Kingdom of Bahrain, September 13–16, 2015.